Spin Drift-Diffusion Boundary Conditions for FEM Modeling of Multilayer SOT Devices

Nils Petter Jørstad*,†,‡, Wolfgang Goes§, Siegfried Selberherr†, and Viktor Sverdlov†,‡
† Christian Doppler Laboratory for Nonvolatile Magnetoresistive Memory and Logic at the
‡ Institute for Microelectronics, TU Wien, Gußhausstraße 27-29, A-1040 Wien, Austria
§ Silvaco Europe Ltd., Cambridge, United Kingdom
* *Email: jorstad@iue.tuwien.ac.at*

***Abstract*—We present results obtained from solving the drift-diffusion equations for spin transport with the finite element method in a ferromagnet/heavy metal/ferromagnet (FM/HM/FM) trilayer, using boundary conditions which account for partial absorption of spins at the HM/FM interfaces. We demonstrate the flexibility of the approach by treating different levels of absorption, and by showing that in the limit of full absorption, the results obtained with the boundary conditions agree with the ones obtained from magnetoelectronic circuit theory.**

***Index Terms*—Spin drift-diffusion, Spintronics, SOT-MRAM**

I. Introduction

Spintronics is a rapidly evolving field that has yielded several promising applications in data storage, sensors, quantum computing, and logic devices [1]. One such application is spin-orbit torque magnetoresistive random access memory (SOT-MRAM), which takes advantage of the strong spin-orbit coupling in heavy metal (HM) layers to generate spin currents from charge currents, enabling effective manipulation of the magnetization in adjacent ferromagnetic (FM) layers through SOTs [2].

To aid the development of these devices, efficient models which can realistically capture the spin transport at HM/FM interfaces in multilayer structures are required. A commonly used approach for the boundary conditions is based on magnetoelectronic circuit theory (MCT) [3]–[5], which relates the transverse spin current at the interface to the experimentally measurable spin-mixing conductance $G^{\uparrow\downarrow}$. However, this model assumes complete absorption of the transverse spin current at the interface, disregarding spin precession and dephasing effects inside the FM. In this work, we explore the use of boundary conditions which treat partial absorption at the interface, by allowing a transmission mixing conductance $\Gamma^{\uparrow\downarrow}$ [6], such that the spin transport inside thin FM layers can be properly captured.

In Section II we present the spin current boundary conditions obtained from considering spin-dependent scattering from a magnetic interface. The interface model is simple, however, it captures the core effects of spin-dependent interface scattering, and leaves room for further extension by considering more realistic interfaces and including interfacial spin-orbit coupling, enabling modeling of the Rashba effect [7]. In Section III we present the spin drift-diffusion model which we consider for computing the spin transport and torques in multilayers, and how the boundary conditions are implemented through an effective interface layer. In Section IV we show numerical results for a FM/HM/FM trilayer structure relevant for modern SOT-devices [8], and compare our approach with results of MCT and the assumption of a continuous spin accumulation and current across the interface [5], [9].

II. Boundary Conditions for HM/FM Interfaces

We consider an HM/FM interface at $z = 0$ with the HM layer below ($z < 0$) and the FM layer above ($z > 0$) the interface. We model the interface by assuming a spin-dependent delta potential at the interface [4]:

$$V(\mathbf{r}) = \frac{\hbar^2 k_F}{m_e}\delta(z)\left(u_0 I_{2\times 2} + u_{ex}\boldsymbol{\sigma}\cdot\mathbf{m}\right) \tag{1}$$

u_0 and u_{ex} are the unitless magnitudes of the spin-independent part of the potential and the exchange interaction at the interface, respectively. $\hbar$ is the reduced Planck constant, m_e is the electron mass, and k_F is the Fermi wave number. The vector $\boldsymbol{\sigma}$ contains the Pauli matricies, $I_{2\times 2}$ is the 2×2 identity matrix, and $\delta(z)$ is the Dirac delta function. We consider the scattering of a non-equilibrium Boltzmann density function for spin and charge $g^I_\alpha(z, \mathbf{k})$ incident on the interface, where $\alpha \in \{x, y, z, c\}$ and $\mathbf{k}$ is the wave vector. The indices x, y, z denote the spin polarization density along the Cartesian axes, and c denotes the charge density. By assuming a free electron gas on either side of the interface, and enforcing the continuity of the wave function and probability current, Boltzmann scattering matrices for reflection and transmission $R_{\alpha\beta}$ and $T_{\alpha\beta}$, respectively, can be derived [10].

Following the same derivation procedure as for the drift-diffusion equations, we obtain the spin and charge currents above (0^+) and below (0^-) the interface by integrating the incident and scattered distribution functions over the Fermi surface [10]:

$$\mathbf{j}_z(0^\pm) = \mp\frac{e}{\hbar(2\pi)^3}\int_{\mathrm{FS}} d\mathbf{k}\frac{k_z}{k_F} \times\left[(I - R(\mathbf{k}))\mathbf{g}^{\mathbf{I}}(0^\pm, \mathbf{k}) - T(\mathbf{k})\mathbf{g}^{\mathbf{I}}(0^\mp, \mathbf{k})\right] \tag{2}$$

$\mathbf{j}_z = [\mathbf{j_{sz}}, j_{cz}]^{\mathrm{T}}$ is a vector containing the spin and charge currents along z, $\mathbf{j_{sz}}$ and j_{cz}, respectively, in units of $\mathrm{A/m^2}$.

e is the elementary charge, k_z is the z-component of the wave vector, and I is the 4×4 identity matrix.

We assume that the incoming out-of-plane spin currents behave as if they originate from spin-dependent reservoirs, which implies

$$\mathbf{g}^{\mathbf{I}}(0^{\pm}, \mathbf{k}) = e\boldsymbol{\mu}(0^{\pm}), \tag{3}$$

where $\boldsymbol{\mu}$ is the spin and charge chemical potential vector in units of V [3], [7]. The integration can then be performed over the scattering matrices to obtain conductance tensors for reflection and transmission given by

$$G = \frac{e^2}{\hbar(2\pi)^3} \int_{\mathrm{FS}} d\mathbf{k} \frac{k_z}{k_F} (I - R(\mathbf{k})) \tag{4}$$

and

$$\Gamma = \frac{e^2}{\hbar(2\pi)^3} \int_{\mathrm{FS}} d\mathbf{k} \frac{k_z}{k_F} T(\mathbf{k}), \tag{5}$$

respectively, containing computed mixing-conductances.

We can then express the difference and average of the currents across the interface, in terms the tensors $\Delta G = G - \Gamma$ and $\overline{G} = (G + \Gamma)/2$, respectively. Separating the spin and charge currents we obtain

$$\Delta \mathbf{J_{sz}} = 2\Delta G_{ss} \overline{\boldsymbol{\mu_s}} \qquad \overline{\mathbf{J_{sz}}} = \overline{G_{ss}} \Delta \boldsymbol{\mu_s} + \overline{\boldsymbol{G_{sc}}} \Delta \mu_c \tag{6}$$

$$\Delta j_{cz} = 0 \qquad \overline{j_{cz}} = \overline{G_{cc}} \Delta \mu_c + \overline{\boldsymbol{G_{cs}}} \cdot \Delta \boldsymbol{\mu_s}, \tag{7}$$

where $\Delta\mu_\alpha = \mu_\alpha(0^-) - \mu_\alpha(0^+)$ and $\overline{\mu_\alpha} = [\mu_\alpha(0^-) + \mu_\alpha(0^+)]/2$. The conductance vector $\overline{\mathbf{G_{sc}}}$ ($\overline{\mathbf{G_{cs}}}$) couples the drop in spin (charge) chemical potential to the average charge (spin) current. A factor of $2\mu_B/e$ has been included into the spin tensors $\Delta G_{ss}, \overline{G_{ss}}$ and $\overline{\mathbf{G_{sc}}}$ to convert the spin current into units of A/s, where μ_B is the Bohr magneton.

Without spin-orbit coupling at the interface the spin torque acting on the magnetization at the interface is given by the difference in transversal spin current across the interface: $\mathbf{T_s^{int}} = \Delta \mathbf{J_{sz}^{\perp}}$, where $\perp$ denotes the transverse components. The results from MCT are obtained by enforcing $\mathbf{J_{sz}^{\perp}}(0^+) = 0$ and $\boldsymbol{\mu_s^{\perp}}(0^+) = 0$. The spin torque acting on the FM is then fully described by the transverse spin current at the HM side of the interface: $\mathbf{T_s^{tot}} = \mathbf{J_{sz}^{\perp}}(0^-)$. The computed SOTs can be included into micro-magnetic models based on the Landau–Lifshitz–Gilbert (LLG) equation to describe the magnetization dynamics during the operation of SOT devices [5], [9], [11]. The resulting spin torques can be decomposed into a damping-like and field-like component with the direction $\hat{\mathbf{d}} = \mathbf{m} \times (\hat{\mathbf{p}} \times \mathbf{m})$ and $\hat{\mathbf{f}} = \mathbf{m} \times \hat{\mathbf{p}}$, respectively, where $\mathbf{m}$ is the normalized magnetization and $\hat{\mathbf{p}}$ is the polarization direction of the spin currents generated in the bulk. The names refer to the terms in the LLG equation, which describe prescession of the magnetization around an effective field and the damping towards it.

Equation (6) and (7) can be used to fully describe the currents and torques across the interface. However, with the inclusion of spin-orbit coupling at the interface, additional currents are generated and losses of spin angular momentum to the lattice occur at the interface. In this case a modification and expansion of the boundary conditions is required [7], [12], which is outside the scope of this work.

III. Spin Drift-Diffusion

We model the spin dynamics in FM multilayers by solving the equation of motion for the non-equilibrium spin accumulation $\mathbf{S}$ [5], [9].

$$\frac{\partial \mathbf{S}}{\partial t} = -\nabla \overline{J_s} - D_e \left(\frac{\mathbf{S}}{\lambda_{sf}^2} + \frac{\mathbf{S} \times \mathbf{m}}{\lambda_J^2} + \frac{\mathbf{m} \times (\mathbf{S} \times \mathbf{m})}{\lambda_\phi^2} \right) \tag{8}$$

$(\overline{J_S})_{ij}$ is the spin current tensor in units of A/s, describing the flow of spin polarization i in direction j, $\boldsymbol{m}$ is the normalized magnetization, and D_e is the electron diffusion constant. λ_{sf}, λ_J, and λ_ϕ are the spin-flip, exchange, and dephasing lengths, respectively. Since magnetization dynamics happen at a much shorter time scale than spin dynamics, we solve (8) for a steady state $\partial \mathbf{S}/\partial t = 0$. The term containing λ_ϕ describes the length scale over which the transverse spin components decay in a magnetic region, while λ_J describes the length scale over which the transverse spin components precess around the magnetization direction.

The spin current contains several contributions such as the diffusion of spin accumulation, polarization of charge current by the magnetization of FM layers, and the spin Hall effect in HM layers [5], [9]:

$$\overline{J_s} = -\frac{\mu_B}{e} \beta_\sigma \mathbf{m} \otimes \left(\mathbf{J_C} - \beta_D D_e \frac{e}{\mu_B} \left[(\nabla \mathbf{S})^{\mathbf{T}} \mathbf{m} \right] \right) - D_e \nabla \mathbf{S} - \theta_{\mathrm{SHA}} \frac{\mu_B}{e} \varepsilon \mathbf{J_C} \tag{9}$$

β_σ and β_D are the conductivity and diffusion polarization parameters, respectively, and θ_{SHA} is the spin Hall angle. ε is the Levi-Civita tensor, and $\otimes$ denotes the outer product. For external boundaries not containing an electrode we enforce the condition $\overline{J_s}\mathbf{n} = 0$. The spin torques inside the FM are related to the flux of transverse spin current and are given by [4], [5]:

$$\mathbf{T_s} = -D_e \frac{\mathbf{S} \times \mathbf{m}}{\lambda_J^2} - D_e \frac{\mathbf{m} \times (\mathbf{m} \times \mathbf{S})}{\lambda_\phi^2} \tag{10}$$

To capture the discontinuities across the interface using the standard finite element method (FEM), which imposes a continuous solution, we treat the interface as a thin layer with a finite thickness d. The drop in current across the thin layer can then be expressed as

$$\Delta \mathbf{J_{sz}} = \int_{-d/2}^{d/2} dz \frac{\partial \mathbf{J_{sz}}}{\partial z} \approx \frac{2\Delta G_{ss}}{d} \int_{-d/2}^{d/2} dz \boldsymbol{\mu_s}, \tag{11}$$

where the mean value theorem for integrals was used to approximate the average spin chemical potential across the interface $\overline{\boldsymbol{\mu_s}}$ in (6). Removing the integrals from (11) yields the following expression for the partial derivative of the spin current inside the interface layer:

$$\frac{\partial \mathbf{J_{sz}}}{\partial z} \approx \frac{2\Delta G_{ss}}{d} \boldsymbol{\mu_s} \tag{12}$$

We express the currents in the interface layer in terms of the average ones, and rewrite the spin current in the interface layer

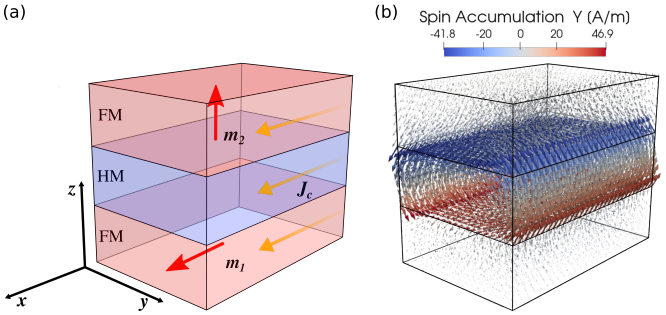

Fig. 1. (a) A FM(4 nm)/HM(4 nm)/FM(4 nm) trilayer oriented along the z-axis, with a constant charge current density along the x-axis. The magnetization of the upper and lower FM is oriented along the z-axis and the x-axis, respectively. (b) The solution of the spin accumulation. The arrows show the orientation of the local spin polarization, while the color bar denotes the magnitude of the y-component.

in terms of charge current by expressing the drop in charge potential $\Delta\mu_c$ in (6) with (7), yielding

$$\mathbf{J_{sz}} \approx d\left[\overline{G_{ss}} - \frac{\overline{\mathbf{G_{sc}}} \otimes \overline{\mathbf{G_{cs}}}}{\overline{G_{cc}}}\right]\frac{\partial \boldsymbol{\mu_s}}{\partial z} + j_{cz}\frac{\overline{\mathbf{G_{sc}}}}{\overline{G_{cc}}}, \qquad (13)$$

where the partial derivative was obtained from the finite difference approximation for the drop in the spin chemical potential $\Delta\boldsymbol{\mu_s}$ in (6).

In order to solve partial differential equations with the FEM, the original equations have to be converted to a weak form. The weak formulation of (8) and (9) is given by [11]. Following the same steps, the weak formulation for the equations in the interface layer is given by

$$\int_{\Omega_{\text{int}}} d\left[\overline{G_{ss}} - \frac{\overline{\mathbf{G_{sc}}} \otimes \overline{\mathbf{G_{cs}}}}{\overline{G_{cc}}}\right]\frac{eD_e}{\mu_B\sigma}\frac{\partial \boldsymbol{S}}{\partial z}\cdot\partial_z\boldsymbol{v}\,d\mathbf{x}$$
$$+\int_{\Omega_{\text{int}}}\frac{2\Delta G_{ss}}{d}\frac{eD_e}{\mu_B\sigma}\boldsymbol{S}\cdot\boldsymbol{v}\,d\mathbf{x} = \int_{\Omega_{\text{int}}} j_{cz}\frac{\overline{\mathbf{G_{cs}}}}{\overline{G_{cc}}}\cdot\boldsymbol{v}\,d\mathbf{x}, \qquad (14)$$

where the spin chemical potential has been expressed in terms of the spin accumulation with the identity $\boldsymbol{\mu_s} = (e/\mu_B)(D_e/\sigma)\mathbf{S}$ [5], σ is the electrical conductivity, and $\mathbf{v}$ is the test function. To obtain the conductance tensors, the scattering matrices R and T are computed analytically [10], and the integrals in (4) and (5) are computed numerically using a standard quadrature scheme for spherical integrals.

IV. Results & Discussion

We solve (8) and (9) on a mesh of the trilayer structure, depicted in Fig. 1(a). We treat the first layer of elements on the FM sides of the boundaries as the effective interface layers, where we solve (12) and (13). The results for the MCT approximation were obtained by setting the elements of (5) corresponding to the transmission conductance to zero, and having a vanishing λ_ϕ inside the FM. A constant charge current density of $5\times10^{12}\text{A}/\text{m}^2$ with the parameters displayed in Tab. I was used to obtain the solution. For the boundary conditions the values $u_0 = 0.42645$, $u_{ex} = 0.20055$ and $k_F = 25.4\ \text{nm}^{-1}$, were used. Fig. 1(b) shows the three-dimensional solution of the spin accumulation in the trilayer

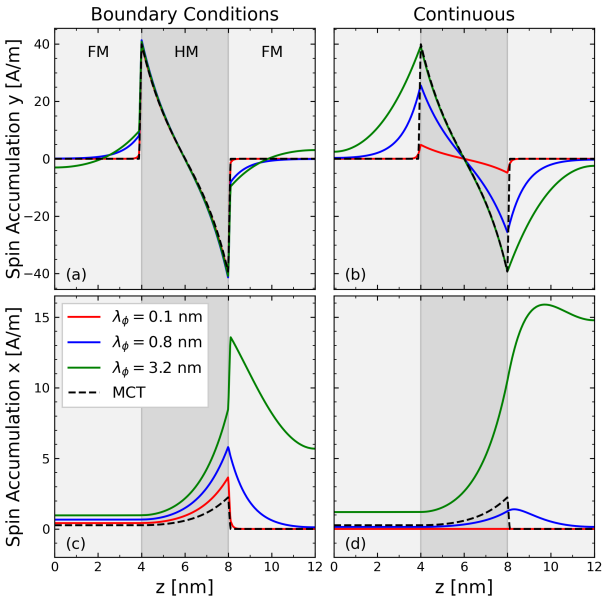

Fig. 2. The solution for the spin accumulation along the z-axis in the center of the trilayer shown in Fig. 1. Panels (a)-(b) and (c)-(d) show the x- and y-components, respectively. Panels (a) and (c) show the results obtained using the boundary conditions, while panels (b) and (d) show the results obtained by treating the currents and accumulations as continuous over the HM/FM interfaces. The dashed lines show results obtain using MCT boundary conditions.

structure, where the spin accumulation generated by the spin Hall effect can be seen in the HM layer.

Fig. 2 shows the solution of the spin accumulation obtained using the boundary conditions or by treating the spin current and accumulation as being continuous across the interface. We observe, that the accumulations obtained by allowing transverse spin currents in FM layers agree with the results of MCT inside the HM layers while allowing for non-zero components inside the FM layers. The x-component corresponding to the field-like direction is shown to increase with increasing spin current penetration. Furthermore, it is shown that the boundary conditions recover the results obtained with MCT for vanishing λ_ϕ, while in the continuous case, they lead to an under- and overestimation of the spin accumulation.

Fig. 3 displays the average spin torque acting on the upper FM. We observe that the boundary conditions produce results which agree well with the results of MCT, except for the considerable increase of the magnitude of the field-like component, consistent with the increase of spin accumulation. For deeply penetrating spin currents ($\lambda_\phi > d_{FM}$), we observe an up to $6\times$ increase in the field-like torque. For the continuous case the resulting torques have a much stronger dependence on the spin penetration, however, depending on the thickness and choice of λ_ϕ, the torques obtained with MCT can be reproduced.

Fig. 4 shows the dependence of the average spin torque on λ_ϕ, where for $\lambda_\phi \to 0$ the torques from MCT are reproduced. Increasing λ_ϕ results in a minor reduction of the damping-like torque and a $4\times$ increase of the field-like torque. In

TABLE I
MATERIAL PARAMETERS

Material↓ / Parameter→	D_e [10^{-3}m^2/s]	σ [MS/m]	β_σ [1]	β_D [1]	λ_{sf} [nm]	λ_J [nm]	θ_{SHA} [1]
FM	1	7	0.42	0.42	42	2.0	-
HM	1.1	7	-	-	1.4	-	0.19

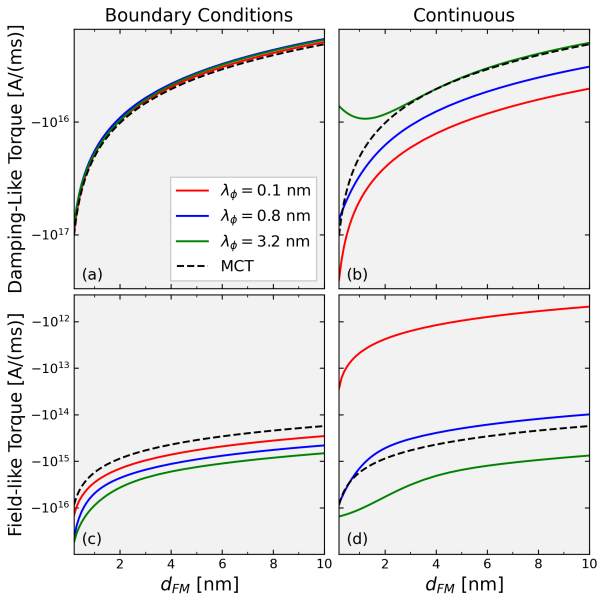

Fig. 3. The average spin torque acting on the magnetization of the upper FM layer, shown in Fig. 1, as a function of the upper FM thickness d_{FM}. Panels (a)-(b) and (c)-(d) show the damping-like and field-like components of the torque, respectively.

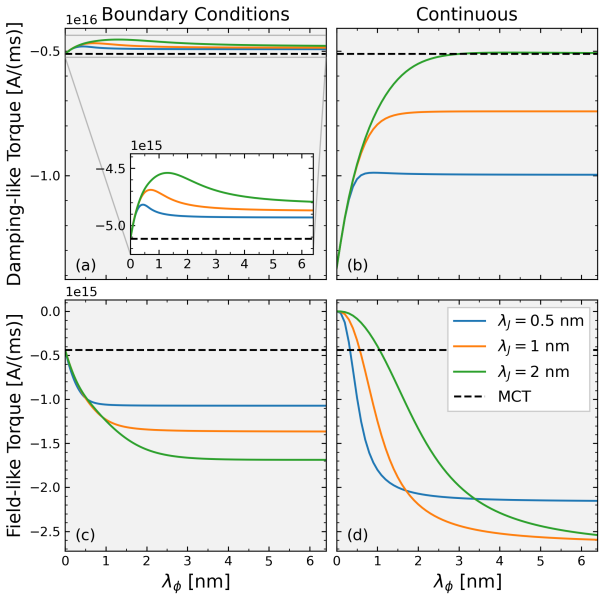

Fig. 4. The average spin torque acting on the magnetization of the upper FM(4 nm) layer, shown in Fig. 1, as a function of the spin dephasing length λ_ϕ. Panels (a)-(b) and (c)-(d) show the damping-like and field-like components of the torque, respectively.

the continuous case we observe that decreasing λ_ϕ leads to a vanishing field-like torque and over-estimated damping-like torque. Decreasing λ_J reduces the torque as spin precession occurs more frequently throughout the FM.

V. CONCLUSION

We demonstrate, that in thin film FM and HM multilayer structures, where transverse spin currents are not fully absorbed, boundary conditions based on quantum mechanical scattering, which can treat partial absorption of spins through HM/FM interfaces, are necessary to properly model the spin transport and torque.

To further investigate spin torques in trilayer structures, the approach can be extended to account for the strong spin-orbit coupling at HM/FM interfaces, which is responsible for the Rashba-Edelstein effect [10].

ACKNOWLEDGMENT

The financial support by the Federal Ministry of Labour and Economy, the National Foundation for Research, Technology and Development and the Christian Doppler Research Association is gratefully acknowledged.

REFERENCES

[1] A. Hirohata, K. Yamada, Y. Nakatani, I.-L. Prejbeanu, B. Diény *et al.*, "Review on spintronics: Principles and device applications," *Journal of Magnetism and Magnetic Materials*, vol. 509, p. 166711, 2020.
[2] Q. Shao, P. Li, L. Liu, H. Yang, S. Fukami *et al.*, "Roadmap of spin–orbit torques," *IEEE Transactions on Magnetics*, vol. 57, no. 7, pp. 1–39, 2021.
[3] A. Brataas, G.E.W. Bauer, and P.J. Kelly, "Non-collinear magnetoelectronics," *Physics Reports*, vol. 427, no. 4, pp. 157–255, 2006.
[4] P.M. Haney, H.-W. Lee, K.-J. Lee, A. Manchon, and M.D. Stiles, "Current induced torques and interfacial spin-orbit coupling: Semiclassical modeling," *Physical Review B*, vol. 87, p. 174411, 2013.
[5] S. Lepadatu, "Unified treatment of spin torques using a coupled magnetisation dynamics and three-dimensional spin current solver," *Scientific Reports*, vol. 7, no. 1, p. 12937, 2017.
[6] M. Zwierzycki, Y. Tserkovnyak, P.J. Kelly, A. Brataas, and G.E.W. Bauer, "First-principles study of magnetization relaxation enhancement and spin transfer in thin magnetic films," *Physical Review B*, vol. 71, p. 064420, 2005.
[7] V.P. Amin and M.D. Stiles, "Spin transport at interfaces with spin-orbit coupling: Formalism," *Physical Review B*, vol. 94, p. 104419, 2016.
[8] K. Cai, G. Talmelli, K. Fan, S. Van Beek, V. Kateel *et al.*, "First demonstration of field-free perpendicular SOT-MRAM for ultrafast and high-density embedded memories," in *International Electron Devices Meeting (IEDM)*, 2022, pp. 36.2.1–36.2.4.
[9] C. Abert, "Micromagnetics and spintronics: models and numerical methods," *The European Physical Journal B*, vol. 92, no. 6, 2019.
[10] V.P. Amin, P.M. Haney, and M.D. Stiles, "Interfacial spin–orbit torques," *Journal of Applied Physics*, vol. 128, no. 15, p. 151101, 2020.
[11] S. Fiorentini, N.P. Jørstad, J. Ender, R.L. de Orio, S. Selberherr *et al.*, "Finite element approach for the simulation of modern MRAM devices," *Micromachines*, vol. 14, no. 5, 2023.
[12] V.P. Amin and M.D. Stiles, "Spin transport at interfaces with spin-orbit coupling: Phenomenology," *Physical Review B*, vol. 94, p. 104420, 2016.